Recent advances in catalysts, palladium alloys and high temperature WGS membrane reactors
A review

CrossMark

Laura Cornaglia, John Múnera, Eduardo Lombardo*

Instituto de Investigaciones en Catálisis y Petroquímica, INCAPE (FIQ, UNL-CONICET), Santiago del Estero 2829, S3006BMF Santa Fe, Argentina

ARTICLE INFO

ABSTRACT

There is an increasing demand for pure H_2 (CO < 10 ppm) to be used in low temperature PEM fuel cells. This puts pressure on the development of alternative routes to purify the hydrogen that is produced in reformers using feedstocks such as natural gas and ethanol. A good option is the water gas shift reaction conducted in a membrane reactor to obtain ultrapure hydrogen. This contribution critically reviews the developments that took place in this decade concerning more efficient, selective, long-lasting catalysts that do not catalyze the formation of methane, graphitic and carbonaceous residues. The membranes, highly selective to hydrogen with high permeability and resistant to poisonous gases, particularly H_2S, are also critically reviewed. Also included in this analysis are the different types of membrane reactors most commonly used.

Introduction

The availability of ultrapure H_2 (<10 ppm CO) at competitive prices is a key factor for the widespread use of PEM fuel cells in stationary and mobile applications. One of the best options to produce this pure gas is through the water—gas shift reaction conducted in a membrane reactor with walls permeable to H_2. To achieve this goal, both good catalysts and membrane materials are needed, which must be accompanied by an efficient reactor design. The two most recent reviews concerning WGSR [1,2] report the state of the art, mapping the literature till 2008 and 2009, respectively. The former [1] provides a broad scope covering from conventional to Pd-based membrane reactors.

The required catalysts should be: i) more active than the commercial ones used in large-scale petrochemical plants for synthesis gas conditioning; ii) non-pyrophoric, non-toxic and of easy start-up able to withstand frequent shutdowns and start-ups without deactivation, especially for mobile applications; iii) highly selective and not catalyzing the formation of methane, carbonaceous residues and graphitic carbon.

The challenges of the development of membrane materials are the following: i) The attainment of H_2 selectivities close to 100% while at the same time operating with the highest possible permeance; ii) Maximum tolerance of H_2S poisoning, a frequent contaminant in industrial feedstocks (e.g. natural gas); iii) Durability at temperatures around 400 °C and retentate pressures of at least 10 bars.

The membrane reactor design should take into account mass and heat transport effects, e.g. to minimize concentration polarization effects and hot spots in the catalytic bed.

All the requirements mentioned above should be met with minimum costs. In what follows, the state of the art in the field of catalysts, membrane materials and high temperature membrane reactors will be critically reviewed.

The catalysts

This work starts with a short summary of Raghavan and co-workers' [2] review concerning catalysts used in membrane reactors. It also includes a brief reference to the options they envisaged at the time concerning the strengths and weaknesses of the formulations studied till 2009 for WGSR, with special emphasis on membrane reactor applications. They compared the commercial high temperature (HT) Fe–Cr and the low temperature (LT) Cu–Zn–Al oxides with the Co, Au and Pt formulations and reached the following conclusions:

- HT and LT commercial catalysts are not useful for membrane reactors, particularly those that require frequent shutdowns as in mobile applications.
- Gold formulations are promissory LT catalysts. This is a novel material that needs further research to evaluate its catalytic behavior more thoroughly. Platinum can be used between 200 and 500 °C. In both cases, their dispersion and stabilities should be improved.
- Sulphur tolerant Co formulations may be worth exploring for LT applications subject to minimization of methane formation.
- Metal-exchanged zeolites should be carefully studied in view of the promising data reported by Desouza et al. [3].

Catalysts of this decade

The evolution of catalysts in the last five years will be discussed in this section. The catalysts will be grouped by the nature of the active metal.

Non-noble metal catalysts
Ni-containing formulations. The main problem of Ni is its ability to catalyze the formation of methane. At least two options have been explored to restrict methanation: i) Addition of alkaline metals such as K [4] and ii) Incorporation of other metals such as Cu [5,6], and Fe [7]. In the first case, small nickel particles were impregnated with a KNO_3 aqueous solution to reach a 5% K load. Both Ni powders with and without K were pelletized, crushed and sieved between 40 and 60 mesh for the catalytic tests. At 350 °C and GHSV of 4000 h^{-1} and 80,000 h^{-1}, the CH_4 selectivity dropped below 0.2% at CO conversions between 99.7 and 86.7% (CH_4 selectivity (%) = (moles of CH_4 produced/moles of CO consumed) × 100). On the basis of CO conversion, Hwang et al. [4] concluded that their catalyst was more active than a Fe–Cr conventional formulation. Although no stability data were provided, it was reported that no coke formation was observed in the used K (5%)/Ni catalyst after 20 h on stream at 350 °C under the most

severe test conditions. Unfortunately, no rate data were provided for comparison with other formulations.

When Ni was alloyed with Cu, a similar quenching of the methanation reaction was observed by Saw et al. [5]. They made a careful characterization of Ni–Cu/CeO_2 formulations covering the whole range of compositions between those of the pure metals. They reported that the best catalyst that did not form methane was the 1:1: Cu:Ni formulation. They showed that this was due to the formation of the Cu–Ni alloy. The XRD patterns of the Cu–Ni catalysts (Fig. 1) show that the alloy was only present in the Cu:Ni = 1:1 (5Cu5Ni) formulation. In the other four Cu–Ni samples studied, only the reflexions of Cu^0 and Ni^0 are seen. It should also be noticed that the alloy containing sample exhibited very strong CO adsorption that sharply limited CO dissociation and, consequently, its methanation. To support these statements they also used EXAFS, H_2-TPR and XPS techniques. Following these findings, Saw et al. [5] aimed further research to a more detailed characterization of the equimolar Cu–Ni supported alloy. In the supplementary data [5], they studied the reaction mechanism and based on their reported data, they concluded that the carboxyl mechanism represents the main pathway of the WGS reaction while the formates are mainly spectators responsible for catalyst deactivation. Another valuable feature of this alloy catalyst is its stability shown in a 100 h on stream experiment run at 400 °C using a feed composition of 5% CO, 25% H_2O and 70% He (H_2O:CO = 5). Under these conditions, the reaction rate was 60.6 μmol of CO converted $g^{-1} s^{-1}$. This value will be later compared with similar catalytic data of Pt formulations (vide infra).

Watanabe et al. [7] showed that the addition of Fe (Ni–Fe/CeO_2) sharply reduces methane formation. At 380 °C, using a feed composition of S/CO = 3.7, 15% CO, 10% CO_2, 60% H_2, N_2
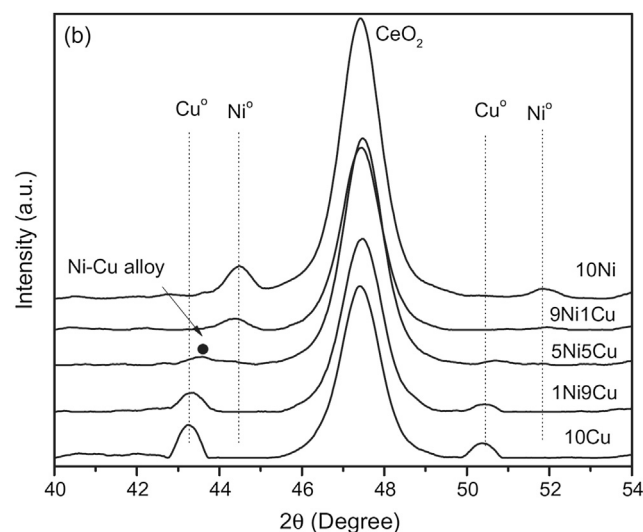

Fig. 1 – **XRD pattern for reduced xNiyCu/CeO_2 catalysts. Reprinted from Journal of Catalysis, 314, Saw ET, Oemar U, Tan XR, Borgna A, Hidajat K, Kawi S., Bimetallic Ni–Cu catalyst supported on CeO_2 for high-temperature water–gas shift reaction: methane suppression via enhanced CO adsorption, 32–46, Copyright (2014), with permission from Elsevier.**

balance (dry basis), they reported near zero methane formation. Unfortunately, they did not provide WGS rate data to compare their catalysts with others reported in the literature. When Re was added to Ni [8], a significant WGS rate increase was reported. They did not say anything concerning methane formation; neither did they provide data concerning stability of the Re–Ni/CeO$_2$ formulation.

Noble metal formulations
Comparison of Au and Pt containing formulations. So far, the main difference between these formulations is that the former can be used at low temperature (ca. 200 °C) while the latter exhibits a wide temperature window (200–500 °C) influenced by the support and the presence of support additives. A very recent publication by González Castaño et al. [9] clearly shows that gold can be more active than Pt at ca. 200 °C but above this temperature Pt rapidly overcomes Au (Fig. 2). Table 1 shows a more complete set of reaction rate data, further supporting the findings of González Castaño et al. [9]. Note that the stability and consequently the activity of Au formulations depend strongly on both the preparation method and pre-treatment conditions employed [13,14]. Furthermore, the Pt formulations are generally more stable than the Au ones.

Pt catalysts. A good starting point for a comparative study of Pt supported on a variety of single and composite oxides is the work of Panagiotopoulou and Kondarides [15]: "A comparative study of the WGS activity of Pt catalysts supported on single (MO$_x$) and composite (MO$_x$/Al$_2$O$_3$, MO$_x$/TiO$_2$) metal oxide carriers". This is a comprehensive study including 13 oxide carriers and 25 composite oxide supports. In all the formulations, they maintained the Pt load constant at 0.5 wt%. In all cases, they checked for the presence of secondary undesirable products, particularly methane. The screening was made with a feed stream of molar composition 3% CO, 10% H$_2$O and 87%
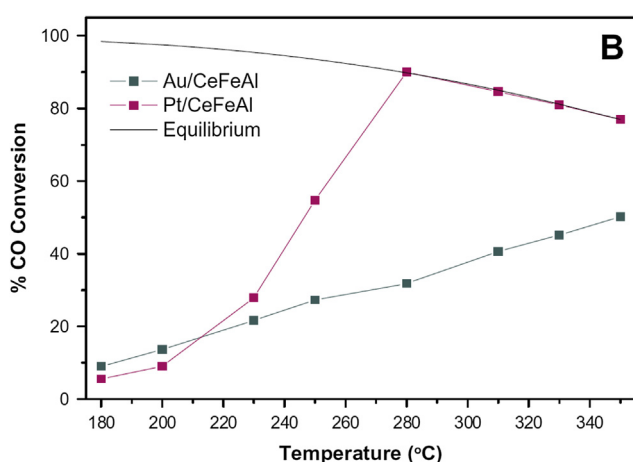
Table 1 – WGS specific reaction rates (mol CO$_{conv}$ g metal^{-1} s^{-1}) of the prepared solids. Reprinted from Journal of Catalysis, 314, González Castaño M, Reina TR, Ivanova S, Centeno MA, Odriozola JA. Pt vs. Au in water–gas shift reaction, 1–9, Copyright (2014), with permission from Elsevier.

Sample	Rate$_{180°C}$ × 10^5	Rate$_{250°C}$ × 10^5
Pt/Al$_2$O$_3$	0.61	8.95
Au/Al$_2$O$_3$	2.07	2.25
Pt/CeO$_2$·Al$_2$O$_3$	2.92	15.54
Au/CeO$_2$·Al$_2$O$_3$	4.91	9.34
Pt/CeO$_2$FeO$_x$Al$_2$O$_3$	4.71	15.69
Au/CeO$_2$FeO$_x$Al$_2$O$_3$	8.94	13.26
Au/CeO$_2$M [10]	4.6	
Au/CeO$_2$ [11]	3.2	
Pt/CeO$_2$ [12]		0.18

He, reaction temperatures (150°–500 °C) and P = 1 bar. The best formulations were then tested with a simulated reformer outlet stream. Because they aimed at LT formulations, they reported reaction rate data at 250 °C in three tables but since they provided apparent activation energies obtained between 170° and 440 °C, values at other temperatures could be estimated.

Table 2 compares the main kinetic data for the less active catalyst Pt/Al$_2$O$_3$ with Pt/TiO$_2$, Pt/CeO$_2$ and composite oxides, all of them with 0.5 wt% Pt load. Note that Pt(0.5%)/CeO$_2$/Al$_2$O$_3$ is ten times more active than Pt(0.5%)/Al$_2$O$_3$. The effect of CeO$_2$ is less noticeable when the more active (TiO$_2$) is the core support material.

The main conclusions from this work are: (i) the increase of the WGS activity of Pt/Al$_2$O$_3$ with the addition of MO$_x$ crystallites may be explained by the positive effect of the oxide reducibility. However, in order to explain why the activity of the composite oxide is higher than Pt/MO$_x$, it is necessary to take into account the MO$_x$ crystallite size as another factor that affects the catalytic activity (Table 2). Note that the reducibility of MO$_x$ increases with smaller crystallite size. (ii) another fact that supports the positive effect of small MO$_x$ crystallite size is the saturation effect observed with increasing MO$_x$ load [15].

Pt/Ce$_x$Zr$_{1-x}$O$_2$. For quite a few years these formulations going from pure CeO$_2$ to pure ZrO$_2$ have been studied as Pt supports for the WGS reaction. In 2011, Vignatti et al. [16] investigated in a systematic way the effect of Zr substitution in CeO$_2$ on the catalytic behavior for the WGSR. They reported that the formulations richer in cerium were the most active ones. They concluded that this was due to a weaker chemisorption of the formate intermediates on cerium rich solids. It has been reported that strong chemisorption of formates are one of the causes of deactivation [2]. This was also reported in the case of WGSR over Rh(0.6%)/La$_2$O$_3$ [17].

Almost simultaneously, Liu et al. [18] studied the WGSR over Pt/CeO$_2$ in the presence of 20 ppm of H$_2$S in the feed stream. They reported that this formulation is quite resistant to sulphur poisoning.

Pt(0.6)/La$_2$O$_3$(27)SiO$_2$. Rh(0.6)/La$_2$O$_3$(27)SiO$_2$ is a highly active, very stable formulation [19] but this is also a methanation

Fig. 2 – Comparison between the catalytic activities: platinum and gold supported on CeFeAl under realistic conditions (9% CO, 30% H$_2$O, 12% CO$_2$ and 50% H$_2$). Reprinted from Journal of Catalysis, 314, González Castaño M, Reina TR, Ivanova S, Centeno MA, Odriozola JA, Pt vs. Au in water–gas shift reaction, 1–9, Copyright (2014), with permission from Elsevier.

Table 2 – Characterization and kinetic data of key Pt(0.5%) catalysts.[a]

Support	SSA[b] (m^2 g^{-1})	Loading (wt%)	D (MO$_x$)[c] (nm)	Pt dispersion (%)	d (Pt)[d] (nm)	Rate at 250 °C (μmol s^{-1} g^{-1})	E$_a$ (Kcal mol^{-1})
Al$_2$O$_3$	83	–	6	84	1.2	0.4	19.2
TiO$_2$	41	–	23	87	1.2	10.3	15.7
CeO$_2$	3.3	–	30	49	2.1	4.9	21.4
CeO$_2$(10)/Al$_2$O$_3$	68	10	8	71	1.4	4.84	21.8
CeO$_2$(10)/TiO$_2$	37	10	6.8	100	1.0	21.1	19.4

[a] Data from P. Panagiotopoulou and D.I. Kondarides [15].
[b] BET area.
[c] Primary crystallite size estimated from XRD broadening.
[d] Mean Pt crystallite size estimated from chemisorption measurements.

catalyst. In runs performed under the same conditions used for the Pt formulation, this catalyst produced 15% CH$_4$ at CO conversions above 90%.

A Pt catalyst was prepared by incipient wetness impregnation of the same binary support using Pt(NH$_3$)$_4$Cl$_2$·H$_2$O as precursor. The XRD patterns showed that the support was made up of La$_2$Si$_2$O$_7$ (very low crystallinity) and amorphous SiO$_2$. Prior to use, the catalyst was heated in Ar at 400 °C and then reduced in situ in flowing H$_2$ at the same temperature for 2 h [20].

Table 3 shows a comparison of the best Pt and Cu:Ni (1:1) catalysts with two commercial Fe–Cr formulations which contain last-generation promoters. The rate data available for this purpose are those obtained using only CO and H$_2$O as reactants. This is so because on the one hand, there are only scarce data reported using feed streams similar to those

coming out of steam reformers and, on the other, the actual compositions used by the authors are different.

Out of the data shown in Table 3 the Pt(0.6%)/La$_2$O$_3$(27)· SiO$_2$ formulation is the second most active and stable of them all, Pt(0.5%)/CeO$_2$(10)/TiO$_2$ being the most active one. However, no stability data are provided for this formulation [15] while the second best catalyst (Pt(0.6)/La$_2$O$_3$(27)SiO$_2$) maintains its activity after the 155 h-long stability test conducted with the start-ups and shut-downs shown in Fig. 3. The Cu–Ni/CeO$_2$ catalyst has been included in this Table because it is a promising formulation using a cheap metal. Note, however, the scarcity of stability data provided in most cases.

One interesting observation is the low Pt dispersion of the Pt(0.6)/La$_2$O$_3$(27)SiO$_2$ formulation. C. Cornaglia et al. [20] tried to check for a possible change of dispersion after use. They

Table 3 – Catalytic behavior of Pt, Ni–Cu and Fe–Cr formulations: HT WGS catalysts.

Catalysts[a]	D[b] (%)	Stability (400 °C) TOS (h)	Decay (%)	Rate[c] 400 °C	Rate[d] 400 °C	H$_2$O/CO	Reference
Pt(0.6)/La$_2$O$_3$(27)·SiO$_2$	16	155[e]	0	170	28.3	1	[20]
	16	155[e]	0	482	80.6	3	[20]
Commercial Fe–Cr with additives	–	[f]	–	40	–	1	[20]
	–	[f]	–	52	–	3	[20]
	–	–	–	42	–	1	[21]
Pt(0.5)/TiO$_2$	67	60	0	290	58.0	3.33	[22]
Pt(0.92)Re(1.79)/Ce$_{0.6}$Zr$_{0.4}$O$_2$	69	60	20[g]	310	33.5	4.5	[23]
Pt(1.05)/Ce$_{0.46}$Zr$_{0.54}$O$_2$	60	60	50[g]	150	14.3	4.5	[23]
Ce$_{0.78}$Sn$_{0.2}$Pt$_{0.02}$O$_{2.5}$ (2.3 wt% Pt)	–	90[h]	0	149[i]	6.48	6.6	[24]
Pt(0.5)/CeO$_2$(10)/TiO$_2$	100	–	–	1300[j]	255[j]	3.3	[25]
Pt(0.5)/CeO$_2$	46	–	–	323[j]	64.6[j]	3.3	[25]
Pt(1.0)/Cr$_2$O$_3$[k]	–	–	–	105[l]	10.5[l]	1	[26]
5Ni:5Cu/CeO$_2$	–			61	–	5	[5]

[a] The weight percent of metals and oxides are indicated between parentheses.
[b] Dispersion.
[c] μmol CO converted. g$_{cat}^{-1}$ s^{-1}.
[d] mmol CO converted. g$_{Pt}^{-1}$ s^{-1}.
[e] No deactivation was observed during start-up/shut-down cycles for at least 155 h (Fig. 2).
[f] Stability of at least one year reported by industry.
[g] Test conducted at 300 °C.
[h] Stability of 90 h reported in Ref. [24] reflects behavior at elevated (>99% conversion).
[i] Extrapolated using E$_{act}$ = 20 kcal mol^{-1} average from Ref. [24].
[j] Calculated from data at 250 °C using the activation energies provided by the authors.
[k] These authors also used as supports: Cr$_2$O$_3$–Fe$_3$O$_4$, CeO$_2$–ZrO$_2$, CeO$_2$, MgO V$_2$O$_5$, ZrO$_2$, Fe$_3$O$_4$, MoO$_3$, MuO$_2$, Al$_2$O$_3$, Bi$_2$MoO$_6$, with 1% Pt. None of these formulations was more active than 1% Pt/Cr$_2$O$_3$.
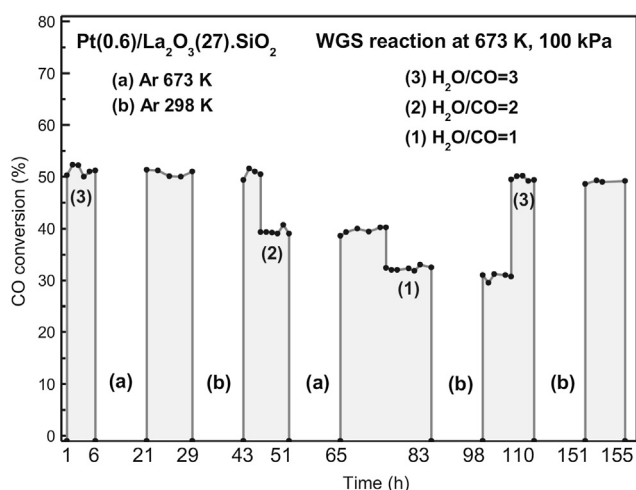[l] Calculated from data at 450 °C using the activation energies provided by the authors.

Fig. 3 – Stability test. CO conversion vs time including start-up and shut-down cycles of WGS reaction over Pt(0.6)/La₂O₃(27)SiO₂ catalyst at 400 °C, 1 bar, H₂O/ CO = 1–3,GHSV = 1.2–1.5 × 10⁶ h⁻¹. Reprinted from Appl Catal A Gen, 462–463, Cornaglia C, Tosti S, Sansovini M, Múnera JF, Lombardo EA., Novel catalyst for the WGS reaction in a Pd-membrane reactor, 278–286, Copyright (2013), with permission from Elsevier.

measured the Pt/Si surface concentration (XPS) before and after reaction and reported no change in this ratio [20] as an indication of no dispersion modification after use. This of course is consistent with the catalytic stability of this formulation (Fig. 3).

One possible explanation of the significant difference in Pt dispersion might be related to the reducibility of the supports, higher in the case of catalysts that chemisorb more H_2 (partly on the support) and, consequently, lead to the higher calculated dispersions shown in Table 3.

Pd(1%)/LaCoO₃. Watanabe et al. [27] impregnated different Pd precursors on a structured $LaCoO_3$ perovskite support. Of the four precursors they used, namely [Pd(NH₃)₄Cl₂, Pd(ethylene-diamine)₂Cl₂, Pd(acetylacetonate)₂, and PdCl₂], the latter was the most effective one. In the four cases, the impregnation steps were repeated until reaching a 1% Pd load on the support. The catalysts were calcined at 550 °C for 2 h. The most active catalyst was washed with different solutions before calcination in order to remove the chloride ligands. The washing agents were water, aqueous solutions of NH_3 or NaOH at pH = 11.05. After immersion in each solution, the structured catalyst was washed with distilled water for 2 min and then calcined at 550 °C for 2 h. The best result was obtained with ammonia washing. Unfortunately, it is not possible to compare the activities of the different formulations with other catalysts reported in the literature because the authors included neither reaction rate and activation energy data nor data concerning the stability of this formulation.

The membranes

The membranes applied in reactors for the WGS reaction were mainly of the inorganic type that can be classified [1] into two

main groups: i) Dense metallic ones: self-supported and composite membranes, ii) Porous membranes.

Recently, Yun and Oyama [28] reviewed the palladium and palladium alloy membranes for hydrogen separation prepared by different fabrication methods and using several supports. They proposed correlations between structure and Pd membrane functions based on mechanistic considerations of permeance along with structural properties and membrane morphologies. In the case of binary palladium-alloys, they proposed that H_2 permeance is generally proportional to the average atomic distances of the alloys. This result is in line with the hydrogen permeation mechanism which is controlled by the diffusion of atomic hydrogen through the metal lattice. A longer atomic distance would facilitate this process.

Several problems in Pd membranes have been identified in the literature: i) embrittlement, ii) deposition of carbonaceous impurities, iii) poisoning by H_2S, iv) high cost and v) low ideal and mixture selectivities.

Membranes based on Pd and Pd alloys

Table 4 summarizes the Pd membranes used in this decade in membrane reactors for the WGS reaction. The composite metallic membranes were synthesized by cold-working (CW), magnetron sputtering (MS), or more frequently by electroless plating (ELP), and their thicknesses were between 3 and 24 μm.

Different configurations and reactor geometries were employed such as tubular and plate-type membranes. In addition, dissimilar scale membranes were applied, including bench scale and Pd films mounted on top of a microchannel configuration.

The main features that have an important effect on MR performance are module design, method of membrane synthesis, hydrogen flux, permeability, feed gas composition, feed pressure, selectivity, stability and the presence of CO, WGS gases and H_2S.

In this review, the discussion has been focused mainly on the latter topics, the inhibition effects of CO, CO_2, WGS mixtures and H_2S on hydrogen permeation through Pd-based membranes. Barreiro et al. [29] classified the gases that can produce a reduction in the hydrogen permeating flux into three main groups on the basis of their interactions with the metal surface: inert gases (Ar, He, N_2), inhibitor gases (CO, CO_2) and poisonous gases (H_2S). The inert gases can build a hydrogen depleted layer adjacent to the membrane surface leading to a concentration polarization effect. In contrast, the inhibitors such as carbon monoxide can adsorb strongly on the membrane surface competing with hydrogen. Basile and coworkers [1] identified CO inhibition as one of the most relevant problems on Pd and Pd-alloy membranes at operating temperatures below 250 °C.

CO inhibition

Different strategies were employed to study the CO and/or CO_2 inhibition effect on hydrogen permeation of Pd membranes. In some cases, the membranes were exposed to H_2/ N_2/CO or H_2/N_2/CO_2 mixtures and in others, experiments, sequences of pure H_2 and pure CO exposures were carried out.

Table 4 – Pd and Pd alloy membranes for H_2 selective separation on WGS membrane reactors.

Membrane	Synthesis method[a]	Thickness (μm)	T(°C)	ΔP(bar)	S_{H_2}[b]	Stability	Gas mixture	Shape, size	Reference
Pd/Al_2O_3	ELP	6	400	7	–	27 days	$CO/CO_2/H_2O/CH_4/H_2$[c]	Bench scale, 44 cm	[37]
Pd/PSS	ELP	24	320−450	5 to 8	S∞	–	H_2/CO_2, $H_2/N_2/CO_2$ $H_2/H_2O/CO_2$	Tube, 70 cm	[29]
PdAg	MS	3	300	3	3000	300 h	$H_2/N_2/CO$	Microchannel	[30]
Pd/PSS	ELP	10.2	350−450	3	S∞	–	H_2, H_2/CO, H_2/CO_2 $H_2/CO/CO_2$[d]	Tube, 7 cm	[31]
Pd/Al_2O_3	ELP	3	300	4.46	2500−3000[f]	20 days	Pure H_2, pure CO[d] WGS simulated stream[e]	Tube, 25 cm	[32]
Pd/PSS	ELP	8−9	350−450	14.7	240−2600	1000 h	H_2 H_2/CO_2 $H_2/CO/CO_2$[d]	Tube, 6 cm	[33]
Pd/PSS	ELP	8−9	400	14.7	240−1200	1000 h	H_2/H_2O[d]	Tube, 6.5 cm	[35]
Pd−Pt/YSZ	ELP	4−12	400	7.7	600−13,000	160 h	H_2, H_2O, CO_2, CO, DOE1[g]	Tube, 13 cm	[36]
PdAu	MS, CW	10−25	400	12.5	–	370 h	WGS simulated stream DOE1, DOE2a, DOE2b[g]	Circular samples	[41]
Pd, PdAu, PdAg PdCu	MS	2	450	–	10,000	100 h	H_2S, WGS simulated stream[h]	Microchannel	[42]
PdAu, PdAgAu/PSS	ELP	4.8−9.3	450−500	11	690−2200	100 h	WGS simulated stream H_2, H_2O, CO_2, CO, H_2S	Tube, 5 cm	[46]

[a] The membranes were synthesized by cold-working (CW), magnetron sputtering (MS) and by electroless plating (ELP).
[b] Ideal selectivity.
[c] $CO/CO_2/H_2O/CH_4/H_2$ = 4.0/19.2/15.4/1.2/60.1.
[d] WGS reaction measurements were carried out.
[e] $H_2/CO/CO_2/CH_4/H_2O$ = 5.22/1/0.48/0.1/2.8, $H_2/CO/CO_2/CH_4$ = 5.22/1/0.48/0.1 and $H_2/CO/CO_2/CH_4/H_2O$ = 6.12/0.1/1.38/0.1/1.9.
[f] Separation factors.
[g] See Table 5.
[h] $H_2/CO_2/H_2O/CO$ = 62/14/20/4.

CO inhibition was investigated by Bredesen and co-workers on a 3 μm thick Pd−Ag alloy membrane at 300 and 350 °C, before and after exposure to air at 300 °C [30]. In this study, the Pd−Ag membrane synthesized by magnetron sputtering was mounted on a microchannel configuration in order to eliminate transport effects. While the hydrogen flux was decreased by ~60% going from 0 to 1 mol% CO (in $H_2/N_2/$ CO mixtures) at 350 °C before heat treatment in air, the reduction was only ~15% after the treatment. They applied an approach combining a Sieverts−Langmuir model equation and microkinetic modeling suggesting that the effect can be explained by changes in CO and H_2 heats of adsorption upon the treatment. The authors attributed the modification in the heats of adsorption to the surface segregation of Pd or Ag due to heat treatment in air.

Permeation measurements with pure gases (H_2 and N_2) and mixtures (H_2 with N_2, CO or CO_2) at several temperatures (ranging from 350 to 450 °C) and trans-membrane pressure differences up to 2.5 bar were carried out by Sanz et al. [31] on Pd membranes prepared by the electroless pore-plating method. The hydrogen permeance, measured when feeding pure hydrogen, decreased for gas mixtures. The complete selectivity was maintained for permeation tests with binary and ternary mixtures of H_2 with N_2, CO and CO_2. Although a detrimental effect on the permeate flux was observed in all cases, the strongest effect occurred in the presence of CO and CO_2 (Fig. 4).

Barreiro et al. [29] investigated the effect of gases such as CO_2, N_2, H_2O on hydrogen permeation through a Pd-based membrane in a bench-scale reactor. They selected different mixtures of H_2/CO_2, $H_2/N_2/CO_2$ and $H_2/H_2O/CO_2$ at temperatures of 320−450 °C and a hydrogen partial pressure of

1.5 bar. Under these conditions, the CO_2 content did not have an important inhibition effect on H_2 permeation. However, they observed that the reverse water gas shift reaction (RWGS) occurred due to the co-existence of H_2 and CO_2. Therefore, the best operating conditions for hydrogen permeation proposed by Barreiro et al. [29] were lower temperatures and water addition to avoid the RWGS and higher feed flow rates.
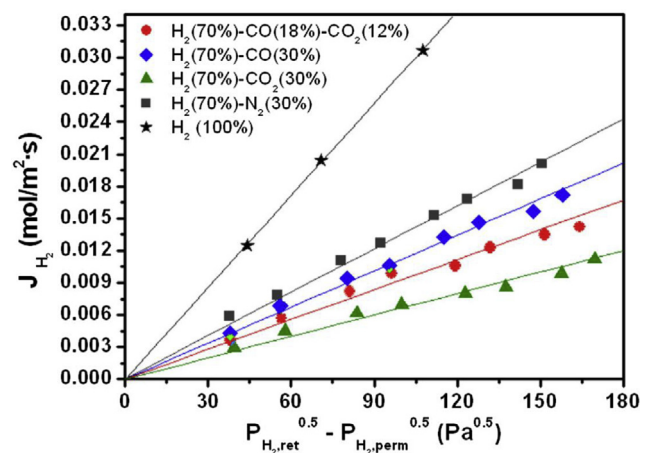

Fig. 4 – **Hydrogen flux versus hydrogen partial pressure with binary and ternary mixtures of H_2 with N_2, CO and CO_2 at 350 °C. Reprinted from Int J Hydrogen Energy, 39, Sanz R, Calles JA, Alique D, Furones L, H_2 production via water gas shift in a composite Pd membrane reactor prepared by the pore-plating method, 4739−4748, Copyright (2014), with permission from Elsevier.**

Ma and coworkers [32] conducted mixed-gas separation experiments on Pd/porous Inconel membranes. The effects of the membrane permeance, gas boundary layer mass transfer resistance, and reversible binding of CO and CO_2 were also considered. Binary mixtures of H_2/He, H_2/CO_2, and a ternary mixture of H_2, CO_2 and CO were fed at 350, 400, and 450 °C and 14.4 bar. The flux of H_2 through the membrane followed Sieverts' law, incorporating the experimentally determined permeance of the Pd-membranes, as well as an inhibition coefficient, η.

$$Pm = \eta Pm_0$$

$$\eta = \frac{1}{1 + A_{CO}P_{CO} + A_{CO_2}P_{CO_2}}$$

where Pm is the permeance of the membrane under mixed gas conditions at high flow rates, Pm_0 is the permeance of the membrane to pure H_2, A_x is the surface interaction parameter for species x on the Pd surface (in inverse pressure units), and P_x is the partial pressure of species x in the gas phase. A similar approach was previously employed by Caravella et al. [33] to model H_2 permeance inhibition by CO through a Pd-membrane. They observed a H_2 permeation inhibition caused by the presence of both CO and CO_2 in the mixtures. The surface interaction parameters, A_{CO} and A_{CO_2}, were calculated based on these data. They found that the value for CO was highly dependent on the temperature, decreasing by 3 orders of magnitude from 350 °C to 450 °C. The surface interaction parameter for CO_2 was small, in agreement with the almost negligible effect of CO_2 on the membrane.

The effect of CO on the H_2 permeation rate through Pd membranes was also experimentally studied by Tsotsis and co-workers [34]. They performed a series of experiments in which the hydrogen flux through the membrane was first measured in a flowing pure hydrogen stream. Following this treatment, the membrane was exposed to a flowing pure CO stream at 300 °C during 3 or 5 h; then, the feed was switched back to pure hydrogen. The hydrogen permeation rate measured after less than five minutes showed no changes. The main difference between these results and the conclusions reported by others [30,31] is related to the type of the experiments (CO mixtures or steps of pure CO).

Water gas shift gases

In addition, Tsotsis and co-workers [34] reported a Pd composite membrane exposed to different mixed-gas, reformate-type feed compositions under sufficiently high feed flow conditions. They calculated the mixed-gas hydrogen permeance by fitting the experimental data; these values were compared with the single-gas permeance for hydrogen measured before and after the experiments. The authors claimed that no systematic trends were observed pointing out detrimental effects (at 300 °C and 3.08 bar) that relate to the presence of CO (or any other reformate mixture component) on the hydrogen permeance.

In order to isolate the effects of H_2O on the supported Pd-membrane as a preliminary to a long-term WGS test, Ma and coworkers [35] tested a porous stainless steel supported thin Pd-membrane under H_2/H_2O (10–37%) mixed-gas conditions for up to 190 h at 400 °C. All the membranes exhibited leak growth under mixed feed conditions at similar rates as those measured during pure H_2 testing, suggesting that the wet atmosphere did not permanently harm the dense Pd-layer. The authors noticed that a significant part of the leak growth was due to defects inherent to the welded regions of the PSS 316L supports. Besides, a repeated exposure of the Pd-surface to H_2O was not found to be a cause for permanent reduction in the H_2 permeance.

Pd–Pt alloy membranes were fabricated via sequential electroless plating by Way and coworkers [36]. The main focus of this study was to examine if the hydrogen flux was affected in a water–gas shift mixture. The mixture was based on the expected composition of coal-derived syngas after a low temperature WGS reactor. All the binary alloy membranes had lower pure gas hydrogen fluxes than pure Pd membranes with the same thickness. Hydrogen fluxes in the DOE 1 mixture (See Table 5) were compared to hydrogen fluxes in 50% hydrogen/nitrogen mixture instead of pure hydrogen fluxes as the membranes would experience similar hydrogen driving forces, hydrogen depletion, and concentration polarization effects. To discard or minimize any possible concentration polarization effects, the feed flow rate was kept high resulting in low hydrogen recovery (H_2 Permeated/H_2 Produced). When the feed gas was switched to the WGS mixture, the hydrogen fluxes decreased in all cases (Fig. 5). The authors hypothesized that the cause for this decline is that carbon monoxide occupies hydrogen dissociation sites.

Similar experiments were carried out in long Pd membrane tubes of 44 cm by Li et al. [37]. In addition, they examined the inhibition effect of WGS-components on the H_2 permeation at near practical working conditions: 400 °C, 20–35 bar feed pressure and 30–90 NL/min feed flow rate with a WGS composition representing the reformate gas from an oxygen-fed autothermal reformer followed by a shift reactor. They observed a H_2 flux drop of ca. 20% compared to H_2/N_2 mixtures with the same H_2 mole fraction, which was enhanced with increasing feed pressure.

The effect of H_2S

The effect of H_2S, a common component of fossil-derived syngas, on Pd based membranes has also been reported in the literature. H_2S can block hydrogen dissociation sites and cause Pd-sulfide formation, which has a lower hydrogen permeability than Pd [38]. Alloying Pd with one or more components such as Au or Cu has been employed to improve its response to H_2S. Most of the literature reports have been focused on H_2S/H_2 mixtures [39,40] and only a few of them studied the effect of the water gas shift mixture containing H_2S.

Table 5 – Feed gas composition (mol %) for WGS mixtures[a] [41].			
Gas	DOE 1	DOE 2A	DOE 2b
H_2	50.0	51.0	33.3
CO_2	30.0	29.0	40.3
H_2O	19.0	19.0	25.3
CO	1.0	1.0	1.3
H_2S	0	20/50[b]	30[b]

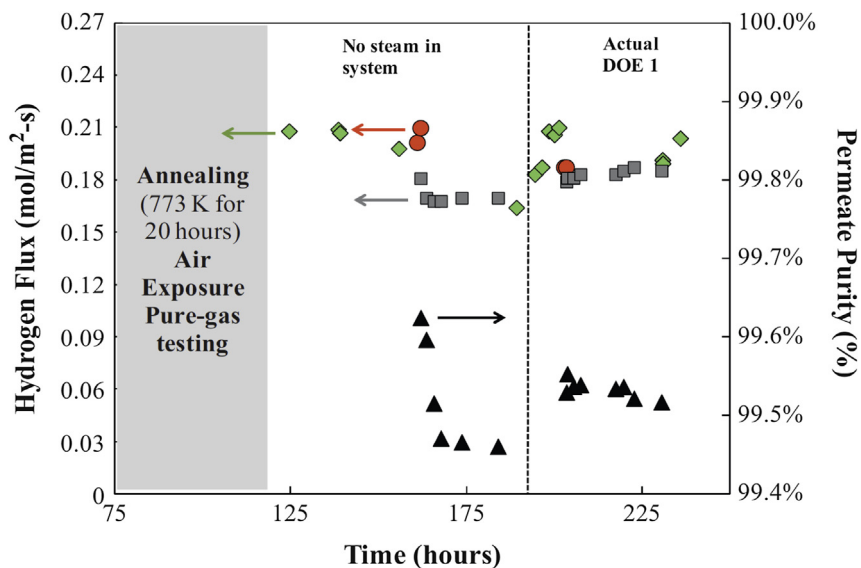[a] Temperature = 400 °C, Pressure = 12.5 bar.
[b] Concentration in ppm.

Fig. 5 – Hydrogen flux with time during mixed-gas testing at 400 °C and feed pressure of 6.9 bar for a Pd-9Pt membrane. Reprinted from Journal of Membrane Science, 427, Lewis AE, Kershner DC, Paglieri SN, Slepicka MJ, Way JD, Pd–Pt/YSZ composite membranes for hydrogen separation from synthetic water–gas shift streams, 257–264, Copyright (2013), with permission from Elsevier.

Way and coworkers [41] focused on PdAu membranes employing two different fabrication techniques to produce more homogeneous distributions of alloy components: magnetron sputtering and cold-working. They tested these materials under simulated water–gas shift streams, with and without H_2S (DOE2a and DOE1) and attempted to both explain and optimize performance under these conditions. Sputtered membranes failed rapidly, while cold-worked membranes maintained acceptable hydrogen selectivity for above 350 h under WGS mixtures containing sulfur compounds. XRD showed that three additional solid compounds were formed during mixture gas testing: two palladium sulfides, Pd_4S and $Pd_{2.8}S$ and a palladium hydride. However, the authors attributed the failure observed in sputtered membranes to metal loss. The mechanism proposed was corrosion spalling, in which the large palladium sulfides formed flaked off. In the case of cold-worked membranes, although sulfidation occurred, it was self-limiting, halting when the remaining metallic Pd–Au was sufficiently gold enriched so that sulfides could no longer form. Membranes with a higher gold content showed less flux inhibition by sulfur containing species. A 20 wt% Au alloy, synthesized by the cold-working technique, had the same permeability in pure hydrogen as it did in a sulfur-free WGS mixture, and only lost 40% of its permeability in a 20 ppm H_2S mixture (Fig. 6). However, the hydrogen purity was 99.83% at the end of testing.

Bredesen and coworkers [42] reported the H_2S exposure and subsequent H_2 flux recovery of pure Pd, Pd77Ag23, Pd85Au15 and Pd70Cu30 membranes. Upon H_2S exposure in H_2/N_2 feed mixtures, all the investigated thin Pd-alloy membranes exhibited a sharp decrease of the H_2 flux depending of the H_2S concentration (2, 20 and 100 ppm). When exposed to a simulated sour WGS mixture, the Pd85Au15 membrane showed an extent of H_2S poisoning about the same magnitude as in WGS mixtures and H_2/N_2 mixtures. No sign of

unselective transport was observed for this membrane after 100 h of operation in a sour WGS mixture.

In contrast to the results reported by Way and coworkers [41], none of the membranes applied, prepared by magnetron sputtering, showed evidence of a decrease in membrane
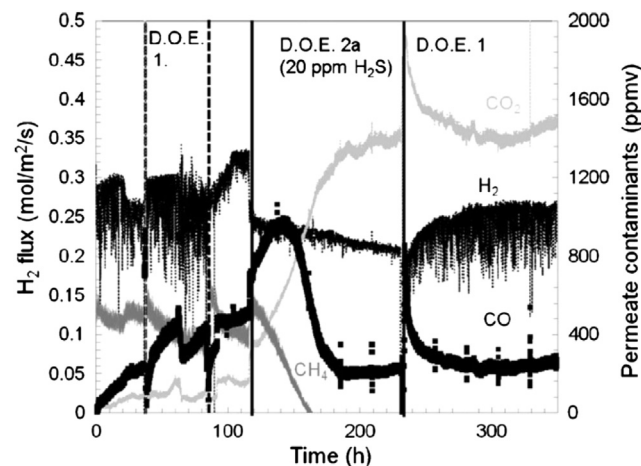

Fig. 6 – Hydrogen flux and permeate contaminant concentrations as a function of time for a cold-worked, 25 μm thick, 20 wt% Au membrane under water–gas shift mixtures at 400 °C, 12.5 bar total feed pressure. Temperature cycles denoted by dashed vertical lines. A 5-point simple moving average was performed on the flux data to minimize noise. Reprinted from Journal of Membrane Science, 378, Gade SK, DeVoss SJ, Coulter KE, Paglieri SN, Alptekin GO, Way JD, Palladium–gold membranes in mixed gas streams with hydrogen sulfide: Effect of alloy content and fabrication technique, 35–41, Copyright (2011), with permission from Elsevier.

thickness. In these membranes, signs of surface roughening combined with grain growth were observed, whilst multiple small pits were found primarily in the grain boundaries of the membrane feed surface after the long-term operation.

Even though Pd-based binary alloys have been extensively studied, latest research has paid attention to ternary Pd alloys for improving both permeability and chemical tolerance [43]. Recently, Braun et al. [44,45] showed that the addition of Au to the high-permeability PdAg binary membrane results in a PdAgAu ternary membrane that minimizes the permanent H_2 flux loss associated with H_2S/H_2 exposure by preventing the formation of thick stable sulfides.

Lewis et al. [46] used electroless deposition to fabricate Pd-23Au and Pd-20Au-13Ag (wt%) composite membranes. Both membranes were tested in a sour WGS mixture containing 20 ppm H_2S at 400 °C and 11 bar feed pressure. The H_2 permeance of the Pd-20Au-13Ag alloy membrane was reduced more than the Pd-23Au one; however, it had a higher absolute H_2 permeance in the sour WGS mixture (Fig. 7). Once the H_2S was removed from the WGS feed gas, the H_2 permeance recovered at least 97% of its original value before H_2S exposure for both membranes. After H_2S testing, sulfides were not detected using XRD. The authors noticed that the values of loss and total recovery were remarkably similar to what was previously reported by Braun et al. [44,45] employing similar PdAgAu alloy compositions. No results of hydrogen permeation or permeance were included in Table 4 since the different mixtures containing H_2, H_2O, CO_2, CH_4, CO and/or H_2S employed made it difficult to attempt a reliable comparison.

Hydrogen production in a membrane reactor

The use of a membrane reactor to perform the water gas shift reaction allows the replacement of the traditional two-unit
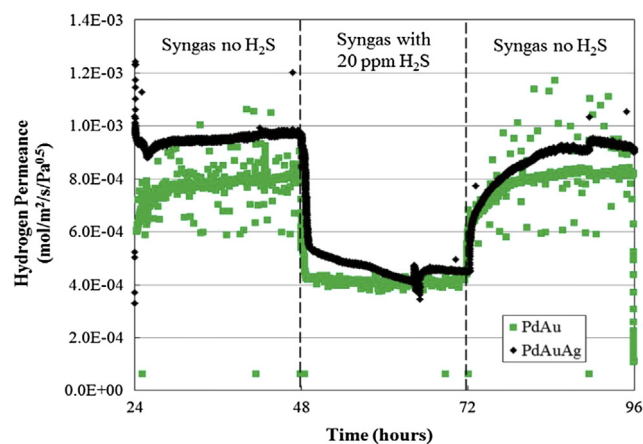

Fig. 7 – Comparison of H_2 permeance of PdAu and PdAuAg alloy membranes in WGS with and without H_2S at a temperature of 400 °C and 1.1 MPa feed pressure. Reprinted from Journal of Membrane Science, 465, Lewis AE, Zhao H, Syed H, Wolden CA, Douglas Way J, PdAu and PdAuAg composite membranes for hydrogen separation from synthetic Water–Gas Shift streams containing hydrogen sulfide, 167–176, Copyright (2014), with permission from Elsevier.

reactor, a unit operated at high temperature (HT) and the other at low temperature (LT), by a one-unit system to obtain high purity H_2 and a CO_2 reach stream. Besides, further purification such as PSA (Pressure Swing Adsorption) or PrOx (Preferential Oxidation of CO) is not needed to reach the low ppm levels required to feed a PEM fuel cell.

In the last few years, there have appeared several reports focusing on the use of membrane reactors to perform water gas shift reaction, but only a few of them have discussed the catalyst-membrane interaction [1,2,47]. Most of these studies used commercial catalysts and only a few operated at high temperatures. Bi et al. [48] employed a noble metal based catalyst $Pt/Ce_{0.6}Zr_{0.4}O_2$ and a Pd membrane reactor to study the WGSR with feeds simulating those obtained by the auto-thermal reforming of natural gas. The authors reported that the CO conversion remained above the thermodynamic equilibrium up to a feed space velocity of 9100 l kg^{-1} h^{-1} at 350 °C, P_{total} = 12 bar and S/C = 3. On the other hand, H_2 recovery decreased from 84.8% at a space velocity of 4050 l kg^{-1} h^{-1} to 48.7% at the highest space velocity. This sharp decline in the separation performance was attributed to a slow H_2 diffusion through the catalyst bed, suggesting that external mass flow resistance has a significant impact on the H_2 permeation rate in such membrane reactors. The authors concluded that in order to obtain an effective H_2 separation/production system, the H_2 recovery can be improved by increasing the operating temperature and/or applying a higher H_2 partial pressure difference between the retentate and permeate sides of the dense PdAg membrane. Mendes et al. [49] studied the influence of the reaction temperature in a range between 200 and 300 °C using a PdAg membrane. Particularly, an increase in CO conversion above equilibrium is more important at higher temperatures (T > 250 °C) due to the larger H_2 removal from the reaction zone.

Cornaglia et al. [20,50] studied this reaction using a PdAg membrane operating at 400 °C; this temperature was imposed by two factors: (i) T < 400 °C increases the CO adsorption on the membrane that reduces the hydrogen permeability, (ii) T > 450 °C reduces the membrane durability because it overtakes the upper operating temperature of the membrane tube brazing and accelerates the formation of pinholes and cracks in the alloy. Thus the optimum temperature of a Pd–Ag membrane reactor conducting the WGS reaction should balance a high CO conversion, a high H_2 recovery and membrane stability.

In order to increase the performance of the membrane reactor, a number of studies [35,48,51,52] analyzed the effect of several operation parameters such as H_2O/CO, temperature, GHSV, pressure and sweep gas flow rate on the CO conversion and H_2 recovery. The best results will be discussed in the next section.

Comparison of WGS membrane reactors performance at high temperatures

Table 5 shows a comparison of the performance of Pd based MRs reported in the literature. This table includes a selection of articles published between 2009 and 2014 showing the best performance of membrane reactors available in the open literature. The reaction temperatures vary between 350 and

Table 6 – Membrane reactor performance for WGS reaction at high temperature.

Membrane	Catalyst	Feed (H₂O/CO)	GHSV (h⁻¹)	Temperature (°C)	Pressure (Bar)	CO Conversion (%)	S_{H_2}[a]	H₂ recovery (%)	Membrane stability (h)	Reference
Pd–Ag/PSS	Fe–Cr	1.6	2900	400	14.4	97	2600	82	1000	[32]
Pd–Ag/PSS	Fe–Cr	1.6	2900	450	14,4	98	2600	84	1000	[32]
Pd/Al₂O₃	Pt (1%)-CeZrO₂	3.0[b]	6250	350	10	95	5000	85	5000	[48]
Pd/PSS	Fe–Cr	1.0	5750	390	10	82	100	56	1000	[51]
Pd/PSS	Fe–Cr	2.5[c]	5650	440	20	84.9	550	42.8	390	[52]
Pd/PSS	Fe–Cr	3.5[d]	1003	410	6	85	300	82	615	[53]
Pd–Ag	Pt (0.6%)-La–Si	2.0	3120	400	8	98	∞	88	>2000	[20]
Pd–Ag	Pt (0.1%)-La–Si	5.0[e]	5100	400	8	92.5	∞	82	>2000	[50]
Pd/Al₂O₃ (Bench scale)	Noble metal	3.8[f]	3000	400	35	92	See text	92	650	[54]

[a]Ideal selectivity.
Feed composition: [b] 34.4% H_2O, 11.8% CO, 7.4% CO_2, 45.3% H_2 and 1.1 CH_4. [c] 51.2% H_2O, 20.5% CO, 8.8% CO_2 and 19.5% H_2. [d] 27.12% H_2O, 7.5% CO, 23.68% CO_2 and 41.7% H_2. [e] 40% H_2O, 8.0% CO, 12% CO_2 and 40% H_2. [f] 15.4% H_2O, 4.0% CO, 19.2% CO_2, 60.1% H_2 and 1.2% CH_4.

450 °C while the retentate pressures go from 3 up to 20 bar. CO conversion (X_{CO}), membrane selectivity, hydrogen recovery and membrane stability are also included as indicators of reactor performance. The reactors were built with either self-standing or composite Pd or PdAg membranes and most of them used commercial Cr–Fe catalysts. Note that a rigorous comparison is not possible due to the wide variety of membrane characteristics, reactor configurations and experimental conditions. Among them, the pressure of the system is especially important since the difference between retentate and permeate pressures constitutes the driving force for the permeation process and, consequently, governs the permeation flux and the reaction equilibrium displacement. In order to maximize the driving force, several authors introduced an inert sweep gas stream in the system [1,20]. However, to facilitate the production of hydrogen with high purity, over-heated steam should be used as sweep gas.

In reference to hydrogen selectivity, most articles provide the ideal selectivity (H_2/N_2) obtained through single component permeation experiments. Concerning H_2 recoveries, Cornaglia et al. [20] reported the highest value employing a self-standing membrane using a pressure difference and a sweep gas as the driving forces for the permeation process. In the case of the composite membranes, other authors applied a pressure difference only. Moreover, in these membranes, the H2 permeated did not reach the purity required to feed PEM fuel cells.

Another aspect to consider is the stability of the membrane. Several studies reported stability data, but few of them clarified whether these studies were performed under reaction conditions.

The results shown in Table 6 were obtained using a H_2O/CO ratio between 1 and 3.5. Several authors studied the effect of the H_2O/CO ratio on CO conversion and H_2 recovery at ca. 400 °C (Fig. 8). Augustine et al. [32] confirmed that higher H_2O/CO ratios led to a higher CO conversion. On the other hand, the H_2 recovery increased for a H_2O/CO ratio between 1 and 1.5 but for higher values the H_2 recovery decreased. This is due to the fact that it depends on both the membrane permeance and CO conversion. The authors reported that the permeance after each measurement decreased due to the carbon formation on

the membrane surface when the reaction was evaluated using a $H_2O/CO = 1$. In the same way, Liguori et al. [51] detected carbon formation after being in reaction at a higher H_2O/CO ratio (3 and 4). The carbon deposition might be due to the Boudouard reaction.

Cornaglia et al. [20] investigated the WGS in membrane reactors using a H_2O/CO ratio between 2 and 3. They employed a Pt-based catalyst that inhibited the carbon formation. Additionally, the hydrogen permeation of the membrane did not change upon the experiments on the membrane reactor; which gave an indication that no carbon contamination of the membrane occurred even though operating at lower H_2O/CO ratios. In brief, steam excess could limit the carbon formation; however, it also reduced the H_2 partial pressure on the reaction side. Besides, Goldbach and coworkers [48] reported that a H_2O excess can be adsorbed on the Pd membrane surface and thus slow down the dissociative adsorption of H_2.

Table 6 also includes results of the bench-scale reactor reported by Jansen and coworkers [54]. The authors reported higher CO conversion (92%) and H_2 recovery (92%) operating at 35 bar pressure. However, the analysis of the retentate stream contained 0.4% N_2 due to the back permeation of sweep N_2
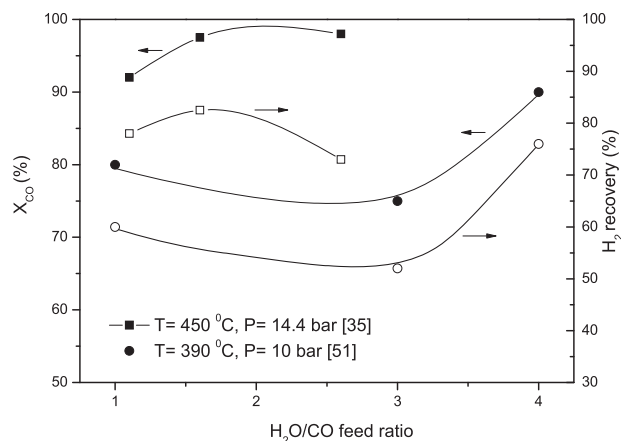

Fig. 8 – Effect of the H_2O/CO ratio on CO conversion and H_2 recovery.

gas. Hence, it can be concluded that the membrane does not have high selectivity to H_2. The authors also reported a high methane formation when the reactor was exposed to a binary CO/H_2 mixture. It is important to remember that a good catalyst for the water gas shift reaction should be highly selective and should not catalyze the formation of carbon or methane.

Reaction tests using feeds with syngas compositions

In the last four years, most articles reported data obtained with feeds of simulated syngas composition, obtained from reforming either natural gas or ethanol. The effect of several operational parameters (temperature, reaction pressure, feed flow rate) in terms of CO conversion and H_2 recovery has been widely addressed [35,48,52,55]. In what follows the effect of the space velocity will be analyzed.

Fig. 9 summarizes several results reported in the literature. Bi et al. [48] studied the influence of the space velocity in a range of 6200 up to 14,000 h^{-1} at 350 °C and 1.2 bar. The authors reported that the CO conversion declined slowly from 96.5% to 94.9% in the entire operation range under study, remaining always above the equilibrium value (90%), indicating a high activity of the catalyst ($Pt/Ce_{0.6}Zr_{0.4}O_2$).

Augustine et al. [32] studied the effects of feed space velocity ($1100-5500 h^{-1}$) at 400 and 450 °C. The authors found two trends. At lower temperature, i.e. at low GHSV, the CO conversion was limited by the driving force of H_2 across the membrane while at high GHSV the CO conversion was limited by the reaction rate and the H_2 permeance. On the other hand, at higher temperature (Fig. 9a), the CO conversion decreased slowly for the whole space velocity range because both the reaction rate and the H_2 permeance are favored at higher temperatures. Liguori et al. [51] observed a similar behavior at higher GHSV values. However, the authors reported a decrease in the hydrogen recovery (Fig. 9b) which could be due to the carbon deposition on the membrane surface. On the contrary, Bi et al. [48] and Augustine et al. [32] concluded that the decrease in the hydrogen recovery is probably due to the short residence time of the reaction mixture in the membrane zone, which reduces the diffusion rate of H_2 from the reactor wall through the catalyst bed to the membrane surface. The mass flow resistance in the catalyst bed has a significant impact on the overall efficiency of the WGS; it could limit the space velocity under which acceptable hydrogen recovery levels can be achieved.

Recently, Catalano et al. [52] studied the influence of the space velocity on reactor performance in a catalytic membrane reactor with a permeation are of 0.02 m^2. They reported that at high GHSV values, using a composite palladium membrane of 7.4 μm thickness, the hydrogen content was depleted less drastically along the membrane length and the concentration polarization phenomenon was less severe due to a better gas transport through the catalytic bed. However, after 390 h of testing, a decline in the membrane selectivity was observed. The authors attributed this decline to the high temperature (440 °C) at which the membrane was exposed.

Stability test of the membrane-catalyst system

The stability of the membrane-catalyst system should be achieved before addressing the possibility of the commercial
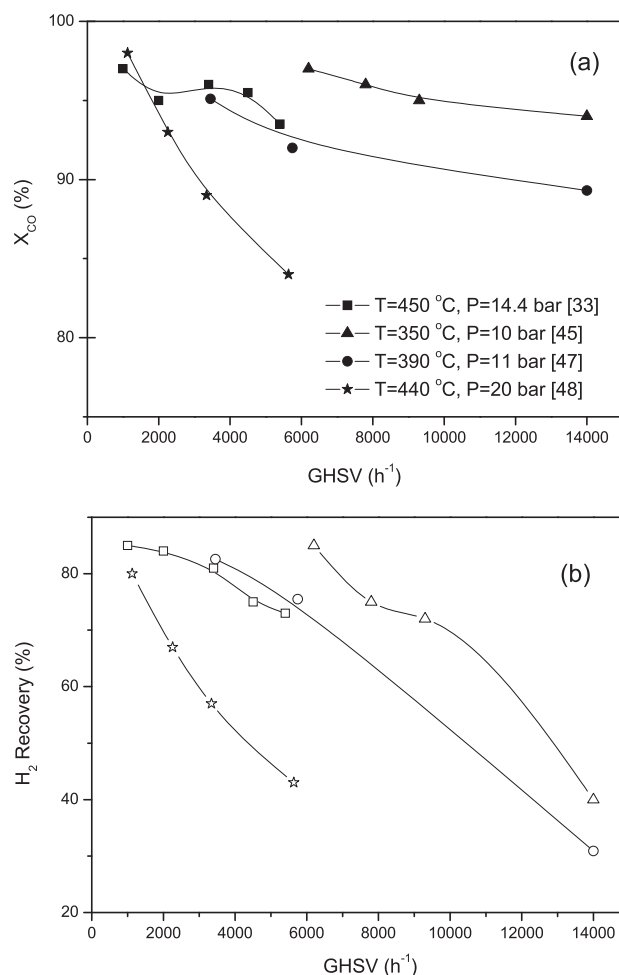

Fig. 9 – Effect of the feed space velocity on CO conversion (a) and H_2 recovery (b). Feed composition: Simulated reforming outlet stream. 45.4% H_2O, 22.7% CO, 9.9% CO_2 and 22% H_2 [32], 34.4% H_2O, 11.8% CO, 7.4% CO_2, 45.3% H_2 and 1.1 CH_4 [48], 32% H_2O, 8% CO, 24% CO_2 and 36% H_2 [51], 51.2% H_2O, 20.5% CO, 8.8% CO_2 and 19.5% H_2.[52].

application of such a system. In the literature there are few studies that report examples of decline in the selectivity of supported Pd-membranes as a result of extended tests under WGS reaction conditions [32,35].

Augustine et al. [32] observed that the H_2 permeance and the selectivity of the membrane, tested after 1175 h in reaction at 450 °C, were lower than before the experiment, due to carbon formation on the membrane surface. The final selectivity of the membrane ($H_2/He = 249$) was still able to produce hydrogen with >99.0% purity under the conditions utilized. Liguori et al. [51], using a Pd based composite membrane, reported a stability of 700 h under reaction conditions. The authors acknowledged the carbon formation in the membrane surface. However, they assumed that the coke deposition was completely reversible. On the other hand, Catalano et al. [52] reported a reduction of 12.7% in hydrogen permeation after 350 h in reaction at 440 °C and 20 bar. Due to the high steam to carbon ratio employed, no carbon formation was observed after the experiments. The authors found that along the axial direction of the membrane appreciable thermal gradients

occurred. Therefore, they concluded that the intermetallic diffusion might have been the main reason for the hydrogen permeance decline.

A long-term testing of a membrane reactor under a fixed set of conditions followed by analysis through microscopic techniques would be necessary to understand gradual changes in membrane performance. In this sense, Augustine et al. [35] studied the durability of PSS-supported membranes under the water gas shift reaction at 400 °C and pressures between 8 and 14.7 bar for a long time on stream (Fig. 10). In the whole operation range, the CO conversion was about 98% and the H_2 recovery was between 80 and 88%. During the last 500 h of operation, the CO concentration on the permeated side increased up to 2600 ppm (Not suitable for PEM cells use). Besides, for practical purposes, it would be interesting to perform a stability test including several start ups and shut downs of the reaction system.

Effect of catalyst mass distribution

Babita et al. [2] mentioned the importance of optimizing the catalyst mass distribution close to the membrane reactor entrance, in order to adjust the membrane separation efficiency considering the excess heat and hydrogen generated. In this section different options are discussed.

Fig. 10 shows three different tubular membrane reactor configurations: packed bed of catalyst enclosed around an inert membrane (Fig. 11a), catalytic bed followed by a membrane in contact with the second part of the catalytic bed (Fig. 11b) and the catalyst supported on the membrane (catalytic membrane) (Fig. 11c). In the first configuration, hot spots may appear in the membrane reactor but this should not be significant since the heat generation during WGSR is small.

One way to control the intensity of hot spots and use a membrane reactor efficiently is to modify the catalyst distribution (Fig. 11b). Drioli and coworkers [55] performed a
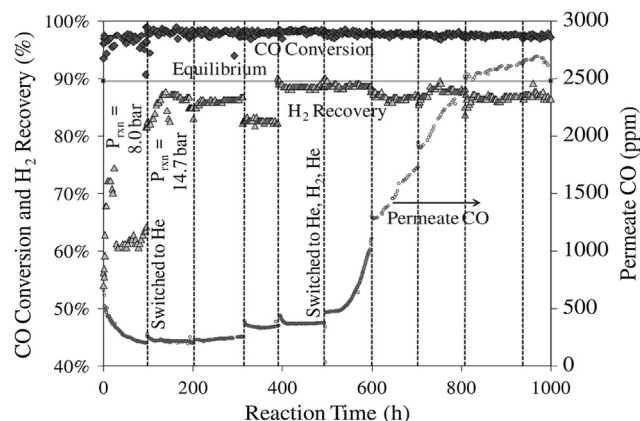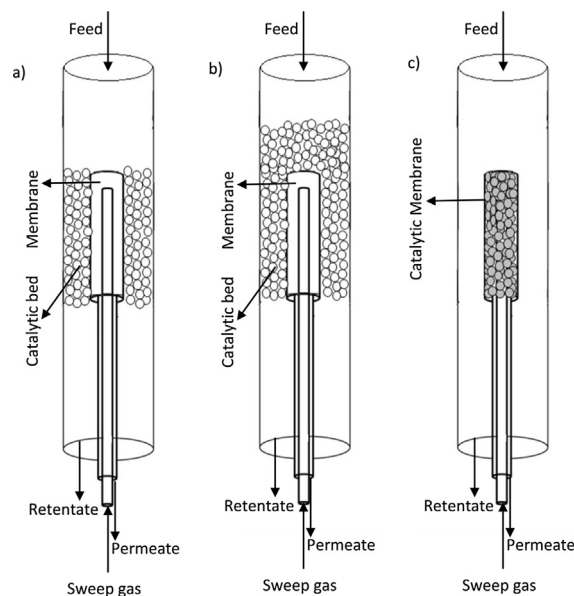

Fig. 11 – Membrane reactor configurations.

theoretical analysis of this effect; the authors concluded that the best configuration is to place a lower catalyst mass where the hot spot occurs and a higher catalyst amount in the zone where the increase of the conversion is negligible. In brief, the reaction starts at the reactor entrance producing H_2 followed by a membrane reactor where the membrane is in contact with the catalytic bed.

The third option is a catalytic membrane (Fig. 11c). Goldbach and coworkers [48] using an inert tubular membrane reported that it is possible to reduce the catalyst bed height and minimize the related external mass transfer resistance if a good catalyst is available. Therefore, with an efficient catalyst supported on the membrane, it is likely that a larger reduction on the mass transfer resistance takes place.

There are no studies published in the open literature that evaluate the WGSR using a catalytic tubular membrane. Recently, Park and coworkers [56] prepared and evaluated a plate-type catalytic membrane reactor equipped with an active nickel metal catalyst and a Pd-based plate-type reactor. Fig. 12 shows the effect of GHSV on CO conversion and H_2 recovery, using two types of membrane reactors (tubular and plate). In the plate type configuration, the CO conversion decreased by 8.1% with the increase of GHSV from 5000 h^{-1}–17,000 h^{-1} while in the case of the tubular-type MR, the CO conversion decreased by 3%. Note that in neither case was a significant decline observed in the CO conversion, compared with the results reported in Fig. 8. In relation to the H_2 recovery in the plate-type catalytic membrane, it decreased only 8.5% while in the tubular membrane reactor it decreased 53%. The authors concluded that the contact between the catalyst and the membrane plates can induce a fast linear flow velocity of the gas decreasing the concentration polarization and favoring the H_2 recovery.

In the literature there are numerous theoretical studies focused on the water gas shift reaction occurring in membrane reactors [2,55,57–59]. In their review, Babita et al. [2] analyzed different mathematical models. The authors
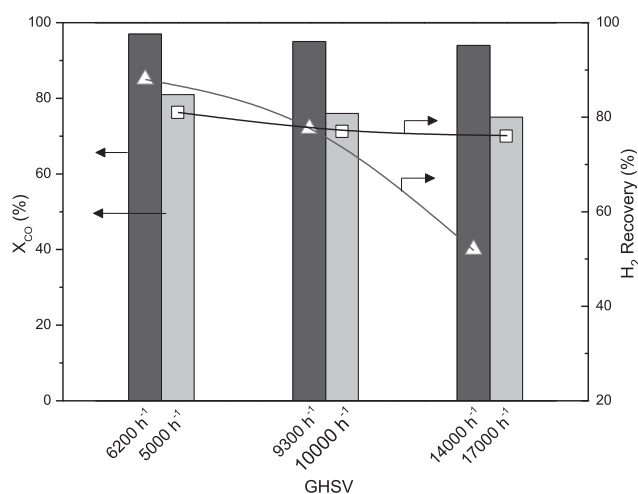

Fig. 10 – Stability test of the WGS using a Pd/PSS membrane. Feed composition: 19% CO, 18% H_2, 8% CO_2 and 55% H_2O; T = 400 °C and GHSV = 2700 h^{-1}. Reprinted from Journal of Membrane Science, 415–416, Augustine AS, Mardilovich IP, Kazantzis NK, Hua Ma Y, Durability of PSS-supported Pd-membranes under mixed gas and water–gas shift conditions, 213–220, Copyright (2012), with permission from Elsevier.

Fig. 12 − Effect of GHSV on the CO conversion and H₂ recovery in two membrane reactor types: plate-type catalytic reactor at 400 °C and H₂O/CO = 2 (Light bar and) [56] and Tubular membrane reactor at 350 °C and H₂O/CO = 3 (Dark bar and Δ) [48].

concluded that it is necessary to develop more advanced reactor models to better simulate the real system behavior. As regards the analysis of operating variables mentioned above, Drioli et al. [55], using a bidimensional mathematical model, studied the effect of catalyst distribution on the performance of a membrane reactor. The simulations results showed that the catalyst mass increasing linearly along the membrane reactor is more efficient than an exponential distribution to control the temperature hot spots. In another study, Ma et al. [59] developed a comprehensive and practical model. The authors studied the effect of different operation variables (temperature, feed flow rate, H₂O/CO ratio, total pressure) on the CO conversion, H₂ recovery and existence of hot spots. On the other hand, with the purpose of avoiding an improper operation of the reactor, several studies [59,60] have analyzed the effect of feed flow with reference to the Damköhler number. This number relates the rate of H₂ formation to the permeation rate of the membrane, making it possible to determine the nature of the controlling step in the membrane reactor, with the help of modeling.

Therefore, thinking about developing a system to be commercially applied, the following features should be considered.

- For practical purposes, it is necessary to perform a stability test including several start-ups and shut-downs of the reaction system.
- It is also necessary to develop WGS catalysts with faster kinetics and a tighter contact configuration between the membrane and the catalyst in membrane reactors.

Conclusions

a) About catalysts
  - There are relatively few studies using reformer outlet compositions as feedstreams.

- Scarce reaction rates and activation energy data have been reported, particularly in the 350–450 °C region.
  - Data concerning catalyst stability are not often reported.
  - Quantitative information concerning methanation activity is especially scant.
  - Only a few studies have reported the poisoning effect of usual contaminants.
b) About the inhibition and poisoning effects on hydrogen permeation through Pd based membranes.
  - A novel approach was proposed to analyze how the Sieverts law is affected by polarization and inhibition by CO.
  - Few studies combining the presence of water gas shift gases and H₂S have been published.
   Pd ternary alloys are the most promising hydrogen selective layers that present an acceptable hydrogen permeability with a high sulfur resistance.
c) About hydrogen production in membrane reactors
  - One way to control the intensity of temperature hot spots to efficiently use a membrane reactor is to optimize the catalyst distribution.
  - The residence time of the reactant affects the hydrogen recovery that it also limited by the catalyst activity and the permeability of the tubular Pd membrane.
  - In a catalytic membrane, the intimate contact between the catalyst and the membrane material decreases the concentration polarization and increases the hydrogen recovery.

The main topics to pay attention to in the coming years should be the following:

- Use of simulated reformer outlet compositions and CO + H₂O for comparison with previous measurements.
- Reaction temperatures between 350 and 450 °C because above ca. 400 °C the negative effect of CO adsorption on H₂ permeation disappears.
- Pressures: 1–15 atm. Higher pressures would require a deeper economic analysis.
- Methane formation data should always be provided.
- Stability tests at least 120 h long with shut-downs and start-ups under controlled conditions in both types of reactors.
- Studies concerning how the water gas shift gases and H₂S affect the hydrogen permeation and catalyst activity.
- Pertinent characterization data of the promising materials.
- Test of synthesis reproducibility of the best catalysts and membranes.
- Adequate high temperature sealings must be used to avoid leakage that will not permit the production of ultrapure hydrogen. Their nature will depend on the materials to be connected (Steel, special alloys, ceramics, etc). A recent publication by Scholes et al. [61] provides an insight into this field. In any case, this is a topic that merits a specialized review.

Acknowledgments

REFERENCES

[1] Mendes D, Mendes A, Madeira LA, Iulianelli A, Sousa JM, Basile A. The water-gas shift reaction: from conventional catalytic systems to Pd-based membrane reactors – a review. Asia Pac J Chem Eng 2010;5:111–37.

[2] Babita K, Sridhar S, Raghavan KV. Membrane reactors for fuel cell quality hydrogen thorugh WGSR – review of their status, challenges and opportunities. Int J Hydrogen Energy 2011;36:6671–88.

[3] Desouza TRO, Brito SMD, Andrade HMC. Zeolite catalysts for the water gas shift reaction. Appl Catal A Gen 1999;178:7–15.

[4] Hwang KR, Lee CB, Park JS. Advanced nickel metal catalyst for water-gas shift reaction. J Power Sour 2011;196:1349–52.

[5] Saw ET, Oemar U, Tan XR, Borgna A, Hidajat K, Kawi S. Bimetallic Ni-Cu catalyst supported on CeO$_2$ for high-temperature water-gas shift reaction: methane suppresion via enhanced CO adsorption. J Cat 2014;314:32–46.

[6] Lin JH, Biswas P, Guliants VV, Misture S. Hydrogen production by water–gas shift reaction over bimetallic Cu–Ni catalysts supported on La-doped mesoporous ceria. Appl Catal A Gen 2010;387:87–94.

[7] Watanabe K, Miyao T, Higashiyama K, Yamashita H, Watanabe M. Preparation of a mesoporous ceria–zirconia supported Ni–Fe catalyst for the high temperature water–gas shift reaction. Catal Commun 2011;12(11):976–9.

[8] Chayakul K, Srithanratana T, Hengrasmee S. Catalytic activities of Re–Ni/CeO$_2$ bimetallic catalysts for water gas shift reaction. Catal Today 2011;175:420–9.

[9] González Castaño M, Reina TR, Ivanova S, Centeno MA, Odriozola JA. Pt vs. Au in water-gas shift reaction. J Catal 2014;314:1–9.

[10] Laguna OH, Centeno MA, Boutonnet M, Odriozola JA. Fe-doped ceria solids synthesized by the microemulsion method for CO oxidation reactions. Appl Catal B Environ 2011;106:621–9.

[11] Dhannia T, Jayalekshmi S, Kumar MCS, Rao TP, Bose AC. Effect of iron dopin and annealing on structural and optical properties of cerium oxide nanocrystals. J Phys Chem Solids 2010;71(7):1020–5.

[12] Brito PCA, Santos DAA, Duque JGS, Macedo MA. Structural and magnetic study of Fe-doped CeO$_2$. Phys B 2010;405(7):1821–5.

[13] Burch R. Gold catalysts for pure hydrogen production in the water–gas shift reaction: activity, structure and reaction mechanism. Phys Chem Chem Phys 2006;8:5483–500.

[14] Haruta M, Yamada N, Kobayashi T, Iijima S. Gold catalysts prepared by coprecipitation for low-temperature oxidation of hydrogen and of carbon monoxide. J Catal 1989;115:301–9.

[15] Panagiotopoulou P, Kondarides DI. A comparative study of the water-gas shift activity of Pt catalysts supported on single (MO$_x$) and composite (MO$_x$/Al$_2$O$_3$, MO$_x$/TiO$_2$) metal oxide carriers. Catal Today 2007;127:319–29.

[16] Vignatti CI, Avila MS, Apesteguía CR, Garetto TF. Study of the water-gas shift reaction over Pt supported on CeO$_2$–ZrO$_2$ mixed oxides. Catal Today 2011;171:297–303.

[17] Cornaglia C, Múnera JF, Cornaglia LM, Lombardo EA, Ruiz P, Karelovic A. Effect of the support on the catalytic stability of Rh formulations for the water-gas shift reaction. Appl Catal A Gen 2012;435–436:99–106.

[18] Liu B, Goldbach A, Xu H. Sour water–gas shift reaction over Pt/CeO$_2$ catalysts. Catal Today 2011;171:304–11.

[19] Cornaglia C, Múnera JF, Lombardo EA. Kinetic study of a novel active and stable catalyst for the water gas shift reaction. Ind Eng Chem Res 2011;50:4381–9.

[20] Cornaglia C, Tosti S, Sansovini M, Múnera JF, Lombardo EA. Novel catalyst for the WGS reaction in a Pd-membrane reactor. Appl Catal A Gen 2013;462–463:278–86.

[21] Lei Y, Cant NW, Trimm D. The origin of rhodium promotion of Fe$_3$O$_4$–Cr$_2$O$_3$ catalysts for the high-temperature water–gas shift reaction. J Catal 2006;239:227–36.

[22] Panagiotopolou P, Kondarides DI. Effects of promotion of TiO$_2$ with alkaline earth metals on the chemisorptive properties and water–gas shift activity of supported platinum catalysts. Appl Catal B Environ 2011;101:738–46.

[23] Choung SY, Ferrandon M, Krause T. Pt-Re bimetallic supported on CeO$_2$-ZrO$_2$ mixed oxides as water–gas shift catalysts. Catal Today 2005;99:257–62.

[24] Gupta A, Hedge MS. Ce$_{0.78}$Sn$_{0.2}$Pt$_{0.02}$O$_{2-\delta}$: a new non-deactivating catalyst for hydrogen production via water–gas shift reaction. Appl Catal B Environ 2010;99:279–88.

[25] Panagiotopolou P, Papavasiliou J, Avgouropoulos G, Ioannides T, Kondarides DI. Water-gas shift activity of doped Pt/CeO$_2$ catalysts. Chem Eng J 2007;134:16–22.

[26] Lei Y, Cant NW, Trimm D. Activity patterns for the 'water gas shift reaction over supported precious metal catalysts. Catal Lett 2005;103:133–6.

[27] Watanabe R, Fujita Y, Tagawa T, Yamamoto K, Furusawa T, Fukuhara C. Pd-supporting LaCoO$_3$ catalytst with structured configuration for water gas shift reaction. Appl Catal A Gen 2014;477:75–82.

[28] Yun S, Oyama TS. Correlations in palladium membranes for hydrogen separation: a review. J Membr Sci 2011;375(1–2):28–45.

[29] Barreiro MM, Maroño M, Sánchez JM. Hydrogen permeation through a Pd-based membrane and RWGS conversion in H$_2$/CO$_2$, H$_2$/N$_2$/CO$_2$ and H$_2$/H$_2$O/CO$_2$ mixtures. Int J Hydrogen Energy 2014;39(9):4710–6.

[30] Mejdell A, Chen D, Peters TA, Bredesen R, Venvik HJ. The effect of heat treatment in air on CO inhibition of a ~3µm Pd-Ag(23wt.%) membrane. J Membr Sci 2010;350(1–2):371–7.

[31] Sanz R, Calles JA, Alique D, Furones L. H$_2$ production via water gas shift in a composite Pd membrane reactor prepared by the pore-plating method. Int J Hydrogen Energy 2014;39(9):4739–48.

[32] Augustine AS, Ma YH, Kazantzis NK. High pressure palladium membrane reactor for the high temperature water–gas shift reaction. Int J Hydrogen Energy 2011;36(9):5350–60.

[33] Caravella A, Scura F, Barbieri G, Drioli E. Inhibition by CO and polarization in Pd-based membranes: a novel permeation reduction coefficient. J Phys Chem B 2010:12264–76.

[34] Abdollahi M, Yu J, Liu PKT, Ciora R, Sahimi M, Tsotsis TT. Ultra-pure hydrogen production from reformate mixtures using a palladium membrane reactor system. J Membr Sci 2012;390–391:32–42.

[35] Augustine AS, Mardilovich IP, Kazantzis NK, Hua Ma Y. Durability of PSS-supported Pd-membranes under mixed gas and water–gas shift conditions 2012. J Membr Sci 2012;415–416:213–20.

[36] Lewis AE, Kershner DC, Paglieri SN, Slepicka MJ, Way JD. Pd–Pt/YSZ composite membranes for hydrogen separation from synthetic water–gas shift streams. J Membr Sci 2013;437:257–64.

[37] Li H, Dijkstra JW, Pieterse JAZ, Boon J, van den Brink RW, Jansen D. Towards full-scale demonstration of hydrogen-selective membranes for CO$_2$ capture: inhibition effect of WGS-components on the H$_2$ permeation through three Pd membranes of 44 cm long. J Membr Sci 2010;363:204–11.

[38] Iyoha O, Enick R, Killmeyer R, Morreale B. The influence of hydrogen sulfide to-hydrogen partial pressure ratio on the sulfidization of Pd and 70 mol% Pd–Cu membranes. J Membr Sci 2007;305:77–92.

[39] Chen C-H, Ma YH. The effect of H$_2$S on the performance of Pd and Pd/Au composite membrane. J Membr Sci 2010;362:535–44.

[40] O'Brien CP, Howard BH, Miller JB, Morreale BD, Gellman AJ. Inhibition of hydrogen transport through Pd and $Pd_{47}Cu_{53}$ membranes by H_2S at 350 °C. J Membr Sci 2010;349:380–4.

[41] Gade SK, DeVoss SJ, Coulter KE, Paglieri SN, Alptekin GO, Way JD. Palladium–gold membranes in mixed gas streams with hydrogen sulfide: effect of alloy content and fabrication technique. J Membr Sci 2011;378(1–2):35–41.

[42] Peters TA, Kaleta T, Stange M, Bredesen R. Hydrogen transport through a selection of thin Pd-alloy membranes: membrane stability, H_2S inhibition, and flux recovery in hydrogen and simulated WGS mixtures. Catal Today 2012;193:8–19.

[43] Peters TA, Kaleta T, Stange M, Bredesen R. Development of ternary Pd-Ag-TM alloy membranes with improved sulphur tolerance. J Membr Sci 2013;429:448–58.

[44] Braun F, Tarditi AM, Miller JB, Cornaglia LM. Pd-based binary and ternary alloy membranes: morphological and perm-selective characterization in the presence of H_2S. J Membr Sci 2014;450:299–330.

[45] Braun F, Miller JB, Gellman AJ, Tarditi AM, Fleutot B, Kondratyuk P, et al. PdAgAu alloy with high resistance to corrosion by H_2S. Int J Hydrogen Energy 2012;37:18547–55.

[46] Lewis AE, Zhao H, Syed H, Wolden CA, Douglas Way J. PdAu and PdAuAg composite membranes for hydrogen separation from synthetic water-gas shift streams containing hydrogen sulfide. J Membr Sci 2014;465(167):176.

[47] De Falco M, Iaquaniello G, Palo E, Cucchiella B, Ciambelli P. Palladium-based membranes for hydrogen separation: preparation, economic analysis and coupling with a water gas shift reactor. Handbook of membrane reactors. Reactor types and industrial applications, vol. 2; 2013. p. 456–86.

[48] Bi Y, Xu H, Li W, Goldbach A. Water–gas shift reaction in a Pd membrane reactor over $Pt/Ce_{0.6}Zr_{0.4}O_2$ catalyst. Int J Hydrogen Energy 2009;34:2965–71.

[49] Mendes D, Chibante V, Zheng JM, Tosti S, Borgognoni F, Mendes A, et al. Enhancing the production of hydrogen via wateregas shift reaction using Pd-based membrane reactors. Int J Hydrogen Energy 2010;35:12596–608.

[50] Cornaglia C, Tosti S, Múnera JF, Lombardo EA. Optimal Pt load of a $Pt/La_2O_3 \cdot SiO_2$ highly selective WGS catalyst used in a Pd-membrane reactor. Appl Catal A Gen 2014;486:85–93.

[51] Liguori S, Pinacci P, Seelamd PK, Keiskid R, Drago F, Calabrò V, et al. Performance of a Pd/PSS membrane reactor to produce high purity hydrogen via WGS reaction. Catal Today 2012;193:87–94.

[52] Catalano J, Guazzone F, Mardilovich IP, Kazantzis NK, Ma YH. Hydrogen production in a large scale water_gas shift pd-based catalytic membrane reactor. Ind Eng Chem Res 2013;52:1042–55.

[53] Pinacci P, Broglia M, Valli C, Capannelli G, Comite G. Evaluation of the water gas shift reaction in a palladium membrane reactor. Catal Today 2010;156:165–72.

[54] Li H, Pieterse JAZ, Dijkstra JW, Boon J, van den Brink RW, Jansen D. Bench-scale WGS membrane reactor for CO_2 capture with co-production of H_2. Int J Hydrogen Energy 2012;37(5):4139–43.

[55] Chiappetta G, Clarizia G, Drioli E. Theoretical analysis of the effect of catalyst mass distribution and operation parameters on the performance of a Pd-based membrane reactor for water–gas shift reaction. Chem Eng J 2008;136:373–82.

[56] Hwang KR, Lee SW, Ryi SK, Kim DK, Kim TH, Park JS. Water-gas shift reaction in a plate-type Pd-membrane reactor over a nickel metal catalyst. Fuel Process Technol 2013;106:133–40.

[57] Adrover ME, Lòpez E, Borio DO, Pedernera MN. Simulation of a membrane reactor for theWGS reaction: pressure and thermal effects. Chem Eng J 2009;154:196–202.

[58] Cornaglia C, Adrover ME, Mùnera JF, Pedernera MN, Borio DO, Lombardo EA. Production of ultrapure hydrogen in a PdeAg membrane reactor using noble metals supported on LaeSi oxides. Heterogeneous modeling for the water gas shift reaction. Int J Hydrogen Energy 2013;38:10485–93.

[59] Koc R, Kazantzis NK, Ma YH. Process safety aspects in water-gas-shift (WGS) membrane reactors used for pure hydrogen production. J Loss Prev Proc 2011;24:852–69.

[60] Brunetti A, Caravella A, Barbieri G, Drioli E. Simulation study of water gas shift reaction in a membrane reactor. J Membr Sci 2007;306:329–40.

[61] Scholes CA, Motuzas J, Smart S, Kentish SE. Membrane adhesives. Ind Eng Chem Res 2014;53:9523–33.